Microelectronics Journal 35 (2004) 731–738

Microelectronics Journal

www.elsevier.com/locate/mejo

Dielectric properties in Au/SnO_2/*n*-Si (MOS) structures irradiated under ^{60}Co-γ rays

N. Tuğluoğlu[a,*], Ş. Altındal[b], A. Tataroğlu[b], S. Karadeniz[a]

[a]*Department of Materials Research, Ankara Nuclear Research and Training Centre, 06100 Beşevler, Ankara, Turkey*
[b]*Department of Physics, Faculty of Arts and Sciences, Gazi University, 06500 Ankara, Turkey*

Received 1 April 2004; revised 23 May 2004; accepted 1 June 2004

Available online 19 July 2004

Abstract

The metal–oxide–semiconductor (MOS) structures with insulator layer thickness range of 55–430 Å were stressed with a bias of 0 V during ^{60}Co-γ ray source irradiation with the dose rate of 2.12 kGy/h and the total dose range was $0–5\times10^5$ Gy. The real part of dielectric constant ε', dielectric loss ε'', dielectric loss tangent $\tan\delta$ and the dc conductivity σ_{dc} were determined from against frequency, applied voltage, dose rate and thickness of insulator layer at room temperature for Au/SnO_2/*n*-Si (MOS) structures from $C–V$ capacitance and $G–V$ conductance measurements in depletion and weak inversion before and after irradiation. The dielectric properties of MOS structures have been found to be strongly influenced by the presence of dominant radiation-induced defects. The frequency, applied voltage, dose rate and thickness dependence of ε', ε'', $\tan\delta$ and σ_{dc} are studied in the frequency (500 Hz–10 MHz), applied voltage (−10 to 10 V), dose rate (0–500 kGy) and thickness of insulator layer (55–430 Å) range, respectively. In general, dielectric constant ε', dielectric loss ε'' and dielectric loss tangent are found to decrease with increasing the frequency while σ_{dc} is increased. Experimental results shows that the interfacial polarization can be more easily occurred at the lower frequency and/or with the number of density of interface states between Si/SnO_2 interfaces, consequently, contribute to the improvement of dielectric properties of Au/SnO_2/*n*-Si (MOS) structures.

Keywords: γ-Rays; Dielectric properties; MOS structure; Radiation effect; Conductivity; Frequency dependence

1. Introduction

The metal–insulator–semiconductor (MIS) or metal–oxide–semiconductor (MOS) structures consist of a semiconductor substrate covered by an insulator layer (such as SnO_2, SiO_2). In MIS structures with thick insulator layer $d_{ox} \le 50$ Å and in MOS structures with thick insulator layer $d_{ox} \ge 50$ Å. These MOS or MIS structures constitute a kind of capacitor which stores the electric charge by virtue of the dielectric property of insulator or oxide layers. Due to its importance in Si technology, the insulator/semiconductor (such as SnO_2/Si, SiO_2/Si) interface and defects on its neighborhood have been extensively studied in the past four decade [1–16]. It has been reported that the most important effects occurring when MOS structures are exposed to radiation [17–29]. Nevertheless, satisfactory understanding in all details has still not been explained in all of the experimental results of the radiation effects on MOS structures. The frequency response of the dielectric constant is dominated by a low-frequency dispersion, whose physical origin has long been in question [30].

When radiation doses greater than a kilorad exposure may cause strong electrical changes in the MOS structures. Because during dose irradiation, large numbers of electron-hole pairs would be generated in the insulator/semiconductor interface. The influence of high-level radiation (e.g. γ-rays, high-level electron, neutrons, and ions) on semiconductor materials produces quasi-stable changes in the characteristics of such materials. For example, the formation of electron-hole pairs begins at higher than 1.02 MeV. For materials with low atomic number Z (such Si and Ge) and for γ-radiation of ^{60}Co, when the MOS structures are stressed with an external bias, these electron-hole pairs would be separated by the strong local internal electric field at grain boundaries. Electrons, which are lighter than that of holes mass, are swept out of

* Corresponding author. Tel.: +90-312-212-6230; fax: +90-312-223-4439.

E-mail address: ntuglu@taek.gov.tr (N. Tuğluoğlu).

0026-2692/$ - see front matter © 2004 Elsevier Ltd. All rights reserved.
doi:10.1016/j.mejo.2004.06.004

the insulator layer quickly by the electric field while the holes move slowly and could be trapped by the defects. So, most of the trapped positive charges would be distributed at the surface of domains.

Recently, wide acceptance has been gained by the capacitance methods of semiconductor investigation, which allows one to obtain an extensive information about the parameters of localized electronic states (or energy levels) [15,16,31,32]. The localized electronic states associated with the surface region were called 'surface states'. A distinction was made between fast and slow surface states, i.e. between states that could exchange charge with the semiconductor space charge region rapidly or slowly, respectively. The slow states were generally thought to be at the outside of the oxide film and the fast ones right at the boundary between the semiconductor and the oxide layer. The reason for their existence is the interruption of the periodic lattice structure at the surface [3,31,33], surface preparation, and formation of insulator layer and impurity concentration of semiconductor [15]. These interface states usually cause a bias shift and frequency dispersion of the capacitance–voltage ($C-V$) and conductance–voltage ($G-V$) measurements [2,3]. To determine the dielectric constant ε', dielectric loss ε'', dielectric loss tangent $\tan\delta$ and the dc electrical conductivity, σ_{dc} of and of Au/SnO_2/n-Si (MOS) structures, the admittance technique [34] was used.

Recently, the radiation response of MOS devices has been found to change significantly when these devices are exposed to irradiation stress treatments [17–29,35]. Winokur et al. [19,25] and Ma [26] were among the first to make a systematic observation of the after irradiation behavior of radiation-induced D_{it} in MOS devices. Especially there are two effects of radiation: the transient effects are due to the electron-hole pair generation and permanent effect is due to the bombardment of devices with radiation which causes changes in the crystal lattice. The radiation-generated holes may diffuse in the insulator, but are less mobile than the electrons; many stationary hole traps are also present.

In our previous study [35], we studied electrical characteristics as well as frequency and radiation dependence of series resistance and density of interface states. We found that the series resistance decreases while the density of interface states increases with increasing dose rate but the series resistance and the density of interface states decrease with increasing frequency. Therefore, in this study, to achieve a better understanding of the effects of different charge surface states on dielectric properties of MOS devices, we measured the $C-V$ and $G-V$ characteristics as a function of γ-ray irradiation doses (0–500 kGy) and oxide thickness for a wide frequency range (500 Hz–10 MHz) at room temperature. The major purpose of this study was to compare estimates of dielectric constant ε', dielectric loss ε'', dielectric loss tangent $\tan\delta$ and dc conductivity σ_{dc} obtained experimentally for Au/SnO_2/n-Si (MOS) structures using $C-V$ and $G-V$ measurements technique in the wide frequency range before and after irradiation.

2. Experimental detail

The MIS structure used in this work was fabricated using n-type (P-doped) single crystals silicon wafer with <111> surface orientation, 280 μm thick, 2″ diameter and 4.45 Ω-cm resistivity. The Si wafer was degreased for 5 min in boiling trichloroethylene, acetone and ethanol consecutively and then etched in a sequence of H_2SO_4 and H_2O_2, 20% HF, a solution of 6HNO_3:1HF:35H_2O, 20% HF. Preceding each cleaning step, the wafer was rinsed thoroughly in de-ionised water of resistivity of 18 MΩ-cm. Immediately after surface cleaning, high purity Au metal (99.999%) with a thickness of 2500 Å was thermally evaporated from the tungsten filament onto the whole back surface of the wafer in the pressure of 1×10^{-6} Torr. Sintering the evaporated Au back contact was formed from the ohmic contact under vacuum. Immediately after ohmic contact, a thin layer of SnO_2 was grown on the Si substrate by spraying a solution consisting of 32.21 wt% of ethyl alcohol (C_2H_5OH), 40.35 wt% of de-ionised water (H_2O) and 27.44 wt% of stannic chloride ($SnCl_4{\cdot}5H_2O$) on the substrate, which was maintained at a constant temperature of 400 °C. The temperature of the substrates was monitored by chromel–alumel thermocouple fixed on top surface of the substrate. The variation of the substrate temperature during spray was maintained within ±2 °C with the help of a temperature controller. The rate of spraying was kept at about 30 cc/min by controlling the carrier gas flow meter. N_2 was used as the carrier gas. SnO_2 dots were 4 mm in diameter. After spraying process, circular dots of 2 mm in diameter and 2500 Å thick Au rectifying contacts were deposited onto the SnO_2 surface of the wafer through a metal shadow mask in liquid nitrogen trapped oil-free ultra-high vacuum system in the pressure of 1×10^{-6} Torr. Metal layer thickness as well as deposition rates were monitored with the help of a digital quartz crystal thickness monitor. The deposition rates were about 1–3 Å/s. The interfacial oxide layer thickness was estimated to be about 55, 140, 290 and 430 Å from measurement of the oxide capacitance in the strong accumulation region. The $C-V$ and $G-V$ measurements were performed in the dark before and after irradiation at various frequencies (500 Hz–10 MHz) and various radiation dose rates (0–500 kGy) by using HP 4192A LF impedance analyzer (5 Hz–13 MHz). As small sinusoidal signal of 40 mV_{p-p} from the external pulse generator is applied to the sample in order to meet the requirement [3,14].

3. Results and discussion

3.1. Frequency, voltage and thickness dependence of ε', ε'', tanδ and σ_{dc}

Frequency, applied voltage and thickness of insulator layer dependence of dielectric constant ε', dielectric loss ε'', dielectric loss tangent tanδ and dc conductivity σ_{dc} of Au/SnO_2/*n*-Si (MOS) structures were determined in the frequency (500 Hz–10 MHz), applied voltage (−10 to 10 V), and thickness of insulator layer (55–430 Å) range, respectively, at room temperature. The dielectric properties at the different frequency and dose rate, including ε', ε'', tanδ and σ_{dc} are measured at room temperature before and after γ-ray irradiation. The real part of the dielectric constant (ε') of the various frequency was calculated using the measurement capacitance values (C_{ma}) at the strong accumulation region from the relation,

$$\varepsilon' = \frac{C_{ox}}{C_0} \quad (1)$$

where $C_0 = \varepsilon_0(A/d_{ox})$; A is the area of the sample, d_{ox} is the interfacial insulator layer thickness and ε_0 is the permittivity of free space charge ($\varepsilon_0 = 8.85 \times 10^{-14}$ F/cm). Because, in the strong accumulation region, the measurement maximal capacitance of MOS structure correspond to the oxide capacitance ($C_{ma} = C_{ox}$) [3]. The imaginary part of the dielectric loss (ε'') of the various frequency was calculated using the measured conductance values (G_{ma}) at strong accumulation region from the relation,

$$\varepsilon'' = \frac{d_{ox}}{A\varepsilon_0}\frac{G_{ma}}{\omega} \quad (2)$$

where G_{ma} is the conductance of MOS structure at any frequency and strong accumulation region, and ω is the angular frequency. The dc conductivity (σ_{dc}) of the various frequencies was calculated using the measured conductance values (G_{ma}) from the relation

$$\sigma_{dc} = \frac{G_{ma}d_{ox}}{A} \quad (3)$$

The dielectric loss tangent tanδ was calculated from the relation,

$$\tan\delta = \frac{4\pi\sigma_{dc}}{\omega\varepsilon'} \quad (4)$$

The frequency dependence of the ε', ε'' and tanδ for Au/SnO_2/*n*-Si (MOS) structure are shown in Fig. 1(a)–(c), respectively. From the measured values of capacitance and conductance, the values of the ε', ε'' and tanδ were found to have strong voltage and frequency dependent. It is clear that the dielectric constant (ε') and dielectric loss (ε'') show (in Fig. 1(a) and (b)) a decrease with increasing frequency, however, ε'' decreases faster than ε' over the same range frequency. The dielectric constant ε' and dielectric loss ε''

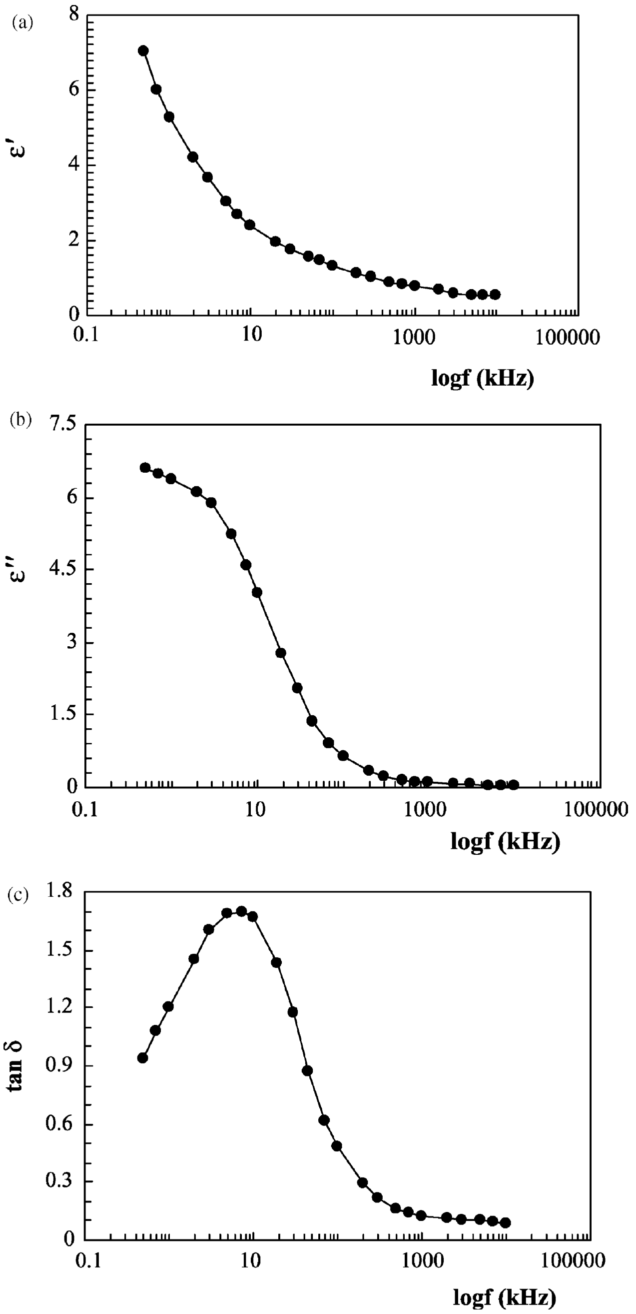

Fig. 1. The frequency dependence of the ε', ε'' and tanδ for Au/SnO_2/*n*-Si (MOS1) structure.

have a values of 7.017, 6.585 at 500 Hz but only 0.76, 0.095 at 1 MHz, respectively. These results shows that the strong low-frequency dispersion that characterizes the frequency dependence of the dielectric constant ε' and dielectric loss ε'' of Au/SnO_2/*n*-Si MOS structure (in Fig. 1(a) and (b)) has never been understood. But in general, four possible mechanism may contribute to low-frequency dielectric behavior of MOS structures; electrode interface, dc conductivity, dipole-orientation and charge carriers [30]. Note that, especially in the high-frequency range (above 1 MHz), the values of ε' become closer to the values of ε''. This behavior of ε' and ε'' may be due to the interface states, cannot follow the ac signal at high-frequency. Such behavior was observed by several authors [30,36–38]. We can see that from Fig. 1(c) while dielectric loss tangent (tanδ) decrease with increasing frequency in the frequency range from 10 kHz to 1 MHz, above at 1 MHz increases with increasing frequency. This behavior can be attributed to the fact that in this frequency range $\varepsilon' = \varepsilon''$.

Signal frequency (f) dependence of $\varepsilon', \varepsilon''$ and tanδ versus V characteristics for the voltage dependence of the ε', ε'' and tanδ for Au/SnO2/n-Si (MOS) structure in the voltage range (-10 to 10 V) are shown in Fig. 2(a)–(d), respectively. As shown in Fig. 2(a)–(c) the values of ε', ε'' and tanδ showed a strong dependence on the applied voltage at various frequency. Fig. 2(a) depicts the dielectric constant against voltage ($\varepsilon' - V$) characteristics obtained for six frequencies. They clearly show two distinctive peaks at the depletion region, further verifying the MOS behavior of the samples, and also indicating the presence of interface trapped charges. These peaks shifted to negative bias and amplitude of peaks decreased with increasing frequency. This fact indicated that the carrier life time of interface trapped charges (τ) are much larger than $1/\omega$ at very high angular frequency (ω), i.e. the charges at interface cannot follow an ac signal. It is clear that the dielectric loss (ε'') shows (in Fig. 2(b)) an increase with increasing voltage. We can see that from Fig. 2(c), almost all frequencies of the dielectric loss tangent (tanδ) decrease with increasing voltage in the voltage range from -10 to 0 V, but above zero-bias, increases with increasing voltage. All tanδ–V curves show a peak and this peak shifted forward to negative bias. These results (in Fig. 2(a) and (b)) are very similar to C–V and G–V characteristics measured from our previous work [35] and Nicollian [31].The thickness of insulator layer dependence of the ε', ε'' and tanδ for MOS structure are shown in Fig. 3(a)–(c), respectively. It is clear that (in Fig. 3(a)–(c) dielectric constant versus thickness of insulator layer ($\varepsilon' - d_{ox}$), dielectric loss–thickness ($\varepsilon'' - d_{ox}$) and dielectric loss tangent–thickness ($tan\delta - d_{ox}$) curves were found to be strongly dependent on insulator layer thickness (d_{ox}). As shown in Fig. 3(a) and (b), ε' and ε'' increases with increasing insulator layer thickness but tanδ decreases with increasing insulator layer thickness. Because the radiation-induced interface state, density increases with increasing thickness of insulator layer [22].

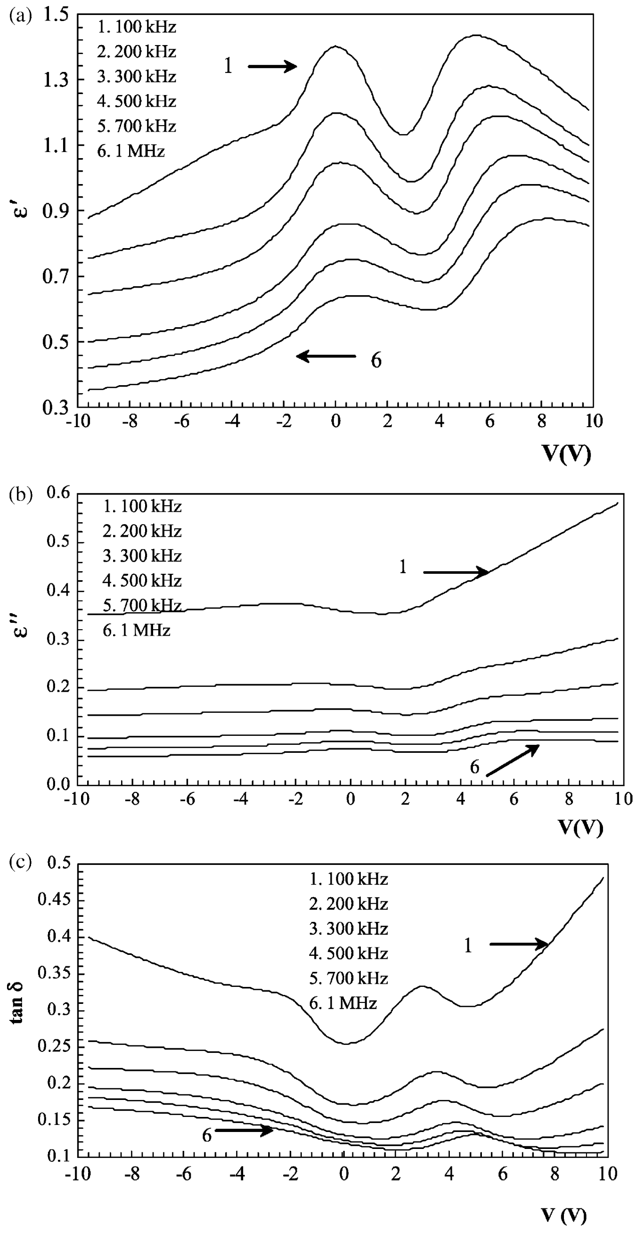

Fig. 2. Signal frequency (f) dependence of the ε', ε'' and tanδ versus V curves for Au/SnO_2/n-Si (MOS1) structure.

The thickness of interfacial oxide layer (d_{ox}) was estimated to be about 55, 140, 290 and 430 Å from measurement of the oxide capacitance in the strong accumulation region ($C_{ma} = C_{ox}$). The frequency, voltage and thickness of insulator layer dependence on dc conductivity (σ_{dc}) are shown in Fig. 4(a)–(c), respectively. Fig. 4(a) depicts the variation of the dc conductivity σ_{dc} with frequency (in the frequency range 500 Hz–10 MHz) at room temperature for Au/SnO_2/n-Si (MOS) structure. It is noticed that the dc conductivity is generally increased with increasing frequency and especially there is a sharp increase in the σ_{dc} above 1 MHz. Below 10 kHz, σ_{dc} seems to be nearly frequency independent or slowly changes, but above 10 kHz, σ_{dc} sharply increases with frequency. Similar behavior was observed in Ref. [36]. This behavior can be attributed to decrease in series resistance with increasing frequency [35]. Fig. 4(b) shows the dc conductivity versus voltage at six frequencies. As shown in Fig. 4(b), the values of dc conductivity showed a strong dependence on the applied voltage. At room temperature, almost every frequency dc conductivity versus voltage curves showed two peaks and these peaks shifted to negative bias but disappear at high frequencies. Fig. 4(c) shows the dc conductivity versus insulator layer thickness at

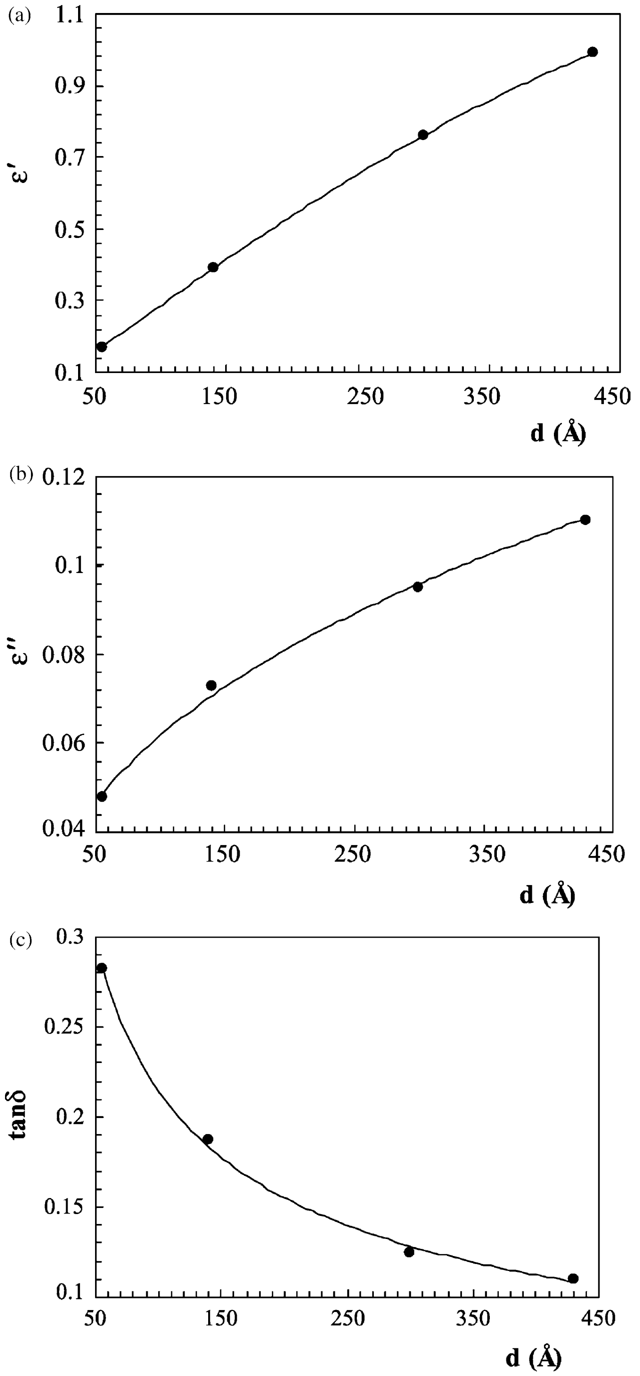

Fig. 3. The dose rate dependence of the ε', ε'' and $\tan\delta$ at 500 kHz for $Au/SnO_2/n$-Si (MOS) structures.

various frequencies. As shown in Fig. 4(c), the values of dc conductivity σ_{dc} increases with thickness of insulator layer.

3.2. Radiation dependence of ε', ε'', $tan\delta$ and σ_{dc}

The dielectric properties at the frequency of 500 kHz, including ε', ε'', $\tan\delta$ and σ_{dc} are measured at room temperature before and after γ-ray irradiation (0–500 kGy). The variation of ε', ε'' and $\tan\delta$ of MOS structure with

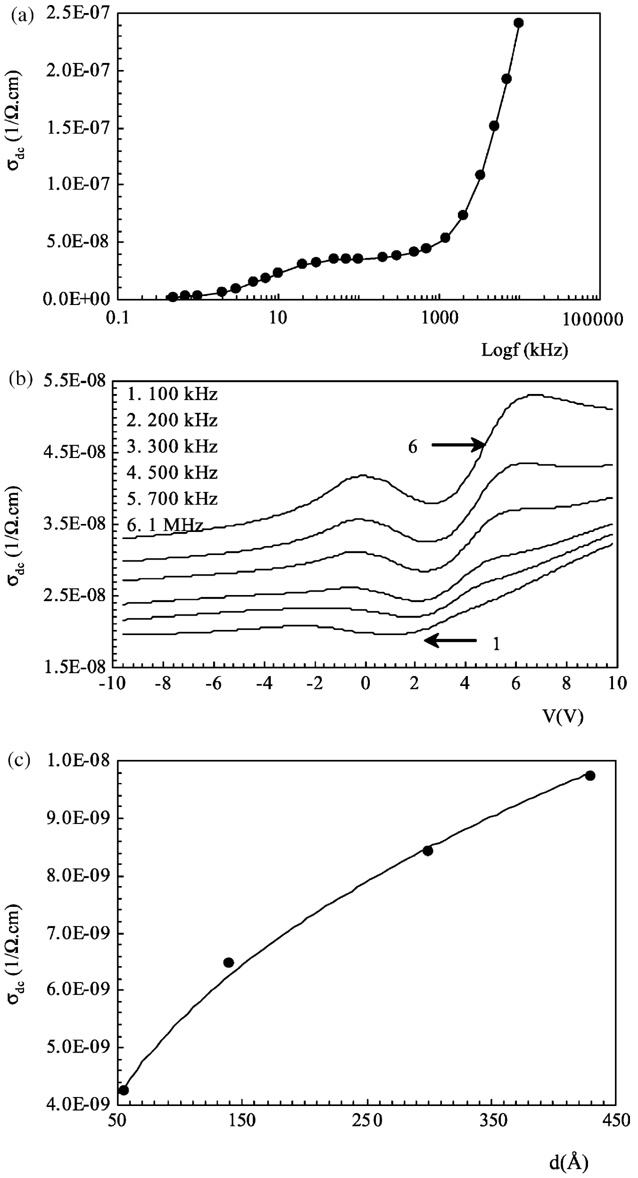

Fig. 4. The frequency and voltage dependence of the conductivity for MOS1 and thickness dependence of the conductivity for $Au/SnO_2/n$-Si structures, respectively.

the absorbed dose are shown in Fig. 5(a)–(c), respectively. It is found that the ε', ε'' and $\tan\delta$ are affected by strong irradiation dose rate. It is noticed that the ε' and ε'' increases with increasing dose rate. However, the dielectric loss tangent $\tan\delta$ decrease with increasing dose rate in the dose range from 0 to 50 kGy, but above 50 kGy, increases with increasing dose rate and than arrives to a constant value after 300 kGy. As shown in Fig. 5, ε' and ε'' are affected little by irradiation up to 300 kGy. Fig. 6 shows the voltage dependence of $\varepsilon' - V$, $\varepsilon'' - V$ and $tan\delta - V$ curves at frequency 500 kHz, respectively. These results are very similar to conductance characteristics (C–V and G–V) measured by Nicollian and Goetzberger [31]. It can be considered that peaks at depletion region are due to

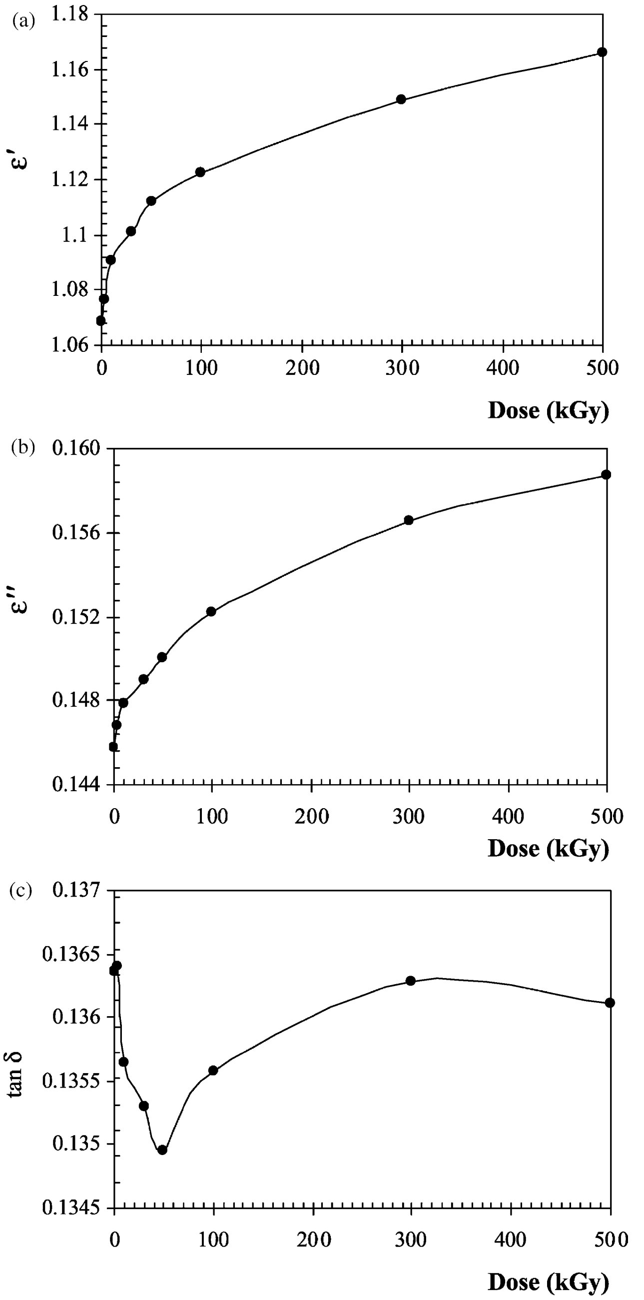

Fig. 5. The variation of the ε', ε'' and $\tan\delta$ of Au/SnO_2/n-Si (MOS1) structures with the absorbed dose at 500 kHz.

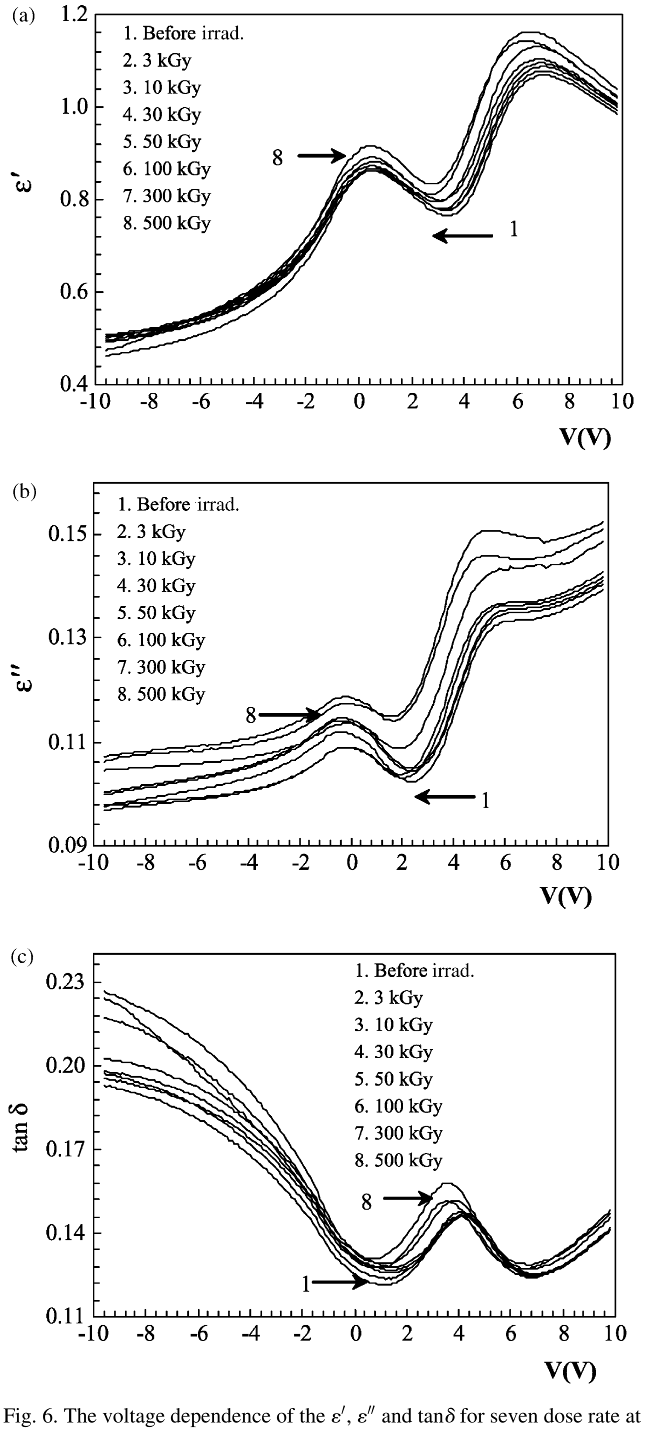

Fig. 6. The voltage dependence of the ε', ε'' and $\tan\delta$ for seven dose rate at 500 kHz for Au/SnO_2/n-Si (MOS) structure.

the interaction between interface states and majority carrier as similar to the explanation on the origin of peak conductance [31]. Because the irradiation on MOS structure became to build up space charge (Q_{sc}) in insulator layer and created the interface trap charge (Q_{it}) at Si–SiO_2 interface. The voltage shift ΔV changes about 1 V with increasing the dose from 0 to 500 kGy. The $\varepsilon' - V$, $\varepsilon'' - V$ and $\tan\delta - V$ curves are quite different for the gate bias. As shown in Fig. 6(a)–(c), the values of ε' and ε'' increase with increasing voltage but $\tan\delta$ decreases with increasing voltage and gives a peak about 4 V. These results suggest that the distribution density of interface state profile is not inherent but a sequence of formation of states at the interface during and after the sample processing.

The voltage and dose rate dependence of dc conductivity obtained for seven dose rate and are shown in Fig. 7(a) and (b), respectively. As shown in Fig. 7(a) the values of dc conductivity showed a strong dependence on the applied voltage and irradiation dose rate for all dose rates. At room

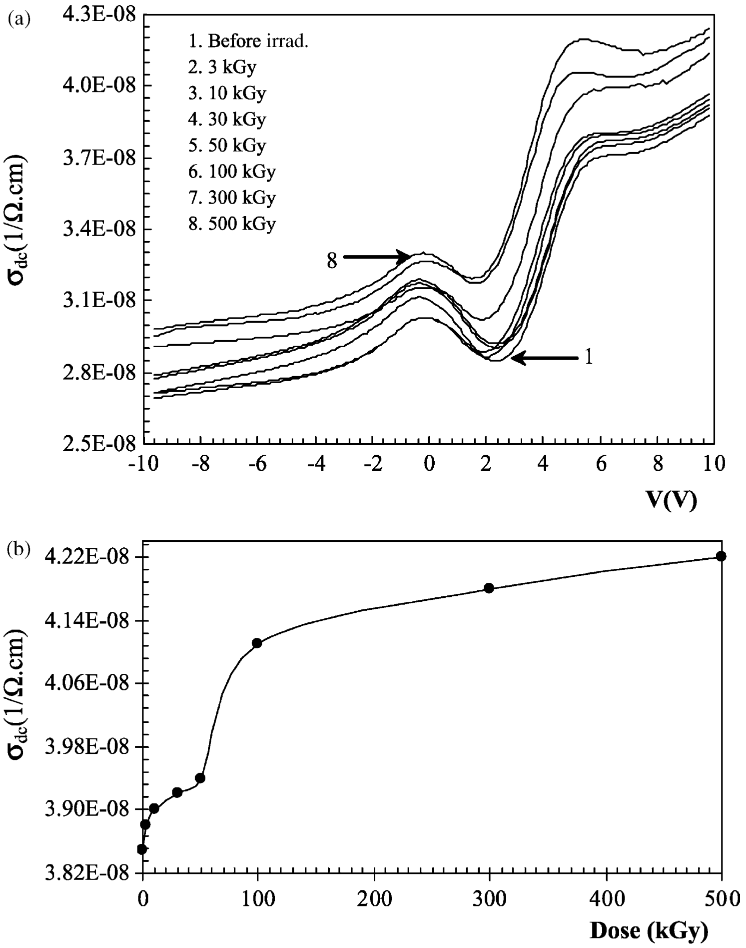

Fig. 7. The voltage and dose rate dependence of the dc conductivity at 500 kHz and in the strong accumulation region for Au/SnO_2/*n*-Si (MOS) structure.

temperature, almost every dose rate dc conductivity versus voltage curves showed two peaks and these peaks shifted to negative bias but the second peak disappears at high dose rate. The observed change in dielectric properties can be understood by considering the displacement damage introduced by irradiation, resulting in the increase in the dielectric constant. The dose rate dependence of dc conductivity obtained for seven dose rate and shown in Fig. 7(b). As shown in Fig. 7(b), dc conductivity (σ_{dc}) is affected little by irradiation up to 100 kGy.

4. Conclusions

From the above studies, we can conclude that the values of real part of dielectric constant ε', dielectric loss ε'', dielectric loss tangent $\tan\delta$ and the dc conductivity of Au/SnO_2/*n*-Si (MOS) structures are strongly dependent on the frequency, applied voltage, dose rate and thickness of insulator layer. The values of ε' and ε'' increase with increasing dose rate, voltage and insulator layer thickness but decrease with increasing frequency. The dc conductivity σ_{dc} increases with increasing dose rate, voltage, insulator layer thickness and frequency. The changes of ε', ε'', $\tan\delta$ and σ_{dc} values are different at different frequency, radiation (γ-ray), voltage and insulator layer thickness range. These results are very significant in the application of the $C-V$ and $G-V$ measurement techniques used in this study. There is an important increase in the conductivity with frequency, voltage and thickness of insulator layer but effect of irradiation than these (f, d_{ox}, γ-ray). The increase in dc conductivity with frequency due to irradiation may be attributed to change centers created. The behavior of dielectric properties strongly depends on frequency, the density of space charges; it is distribution profile, and the thickness of insulator layer. It is also considered that the total interface state density increases with increasing amount of irradiation dose.

Acknowledgements

This work is supported by Turkish Atomic Energy Authority's State Planning Organization Supported Project 'AP2.Nuclear Techniques in Sustainable Development and Environmental Protection' and also by Turkish of Prime Ministry State Planning Organization Project Number 2001K120590.

References

[1] H.C. Card, E.H. Rhoderick, Studies of tunnel MOS diodes I. Interface effects in silicon Schottky diodes, J. Phys. D: Appl. Phys. 4 (1971) 1589–1601.

[2] S. Kar, W.E. Dahlke, Interface states in MOS structures with 20–40 Å thick SiO_2 films on nondegenerate Si, Solid-State Electron. 15 (1972) 221–237.

[3] E.H. Nicollian, A. Goetzberger, MOS conductance technique for measuring surface state parameters, Appl. Phys. Lett. 7 (1965) 216–219.

[4] A. Singh, K.C. Reinhardt, W.A. Anderson, Metal–insulator–semiconductor junctions, J. Appl. Phys. 68 (1990) 3475–3483.

[5] B. Akkal, Z. Benamara, B. Gruzza, L. Bideux, Characterization of interface states at Au/InSb/InP (100) Schottky barrier diodes as a function of frequency, Vacuum 57 (2000) 219–238.

[6] A. Ahaitouf, A. Bath, P. Thevenin, E. Abarkan, Analysis of interface states of n-InP MIS structures based on bias dependence of capacitance and photoluminescence intensity, Mater. Sci. Eng. B77 (2000) 67–72.

[7] M. Schulz, E. Klausmann, Transient capacitance measurements of interface states on the intentionally contaminated $Si–SiO_2$ interface, Appl. Phys. 18 (1979) 169–175.

[8] S. Kar, R.L. Narasimhan, Characteristics of the $Si–SiO_2$ interface states in thin (70–230 Å) oxide structures, J. Appl. Phys. 61 (12) (1987) 5353–5359.

[9] N. Konofaos, I.P. McClean, C.B. Thomas, Characterisation of the interface states between amorphous diamond-like carbon films and (100) silicon, Phys. Status Solidi A 161 (1997) 111–123.

[10] H.S. Haddara, M. El-Sayed, Conductance technique in MOSFETs: of interface trap properties in the depletion and weak inversion regimes, Solid-State Electron. 31 (8) (1988) 1289–1298.

[11] P. Chattopadhyay, A.N. Daw, On the current transport mechanism in a metal–insulator–semiconductor (MIS) diode, Solid-State Electron. 29 (1986) 555–560.

[12] M.K. Hudait, S.B. Krupanidhi, Effects of thin oxide in metal–semiconductor and metal insulator–semiconductor epi-GaAs Schottky diodes, Solid-State Electron. 44 (2000) 1089–1097.

[13] A.H. Heime, H. Pagnia, Influence of the semiconductor-oxide interlayer on the AC-behaviour of InSb MOS-capacitors, Appl. Phys. 15 (1978) 79–84.

[14] K.K. Hung, Y.C. Cheng, Characterization of $Si–SiO_2$ interface traps in p-metal–oxide–semiconductor structures with thin oxides by conductance technique, J. Appl. Phys. 62 (10) (1987) 4204–4211.

[15] S. Özdemir, Ş. Altındal, Interface state density profile in SiO_2/p-Si from conductance measurement, Doğa-Tr, J. Phys. 17 (1993) 838–846.

[16] H. Deuling, E. Klausmann, A. Goetzberger, Interface states in $Si–SiO_2$ interfaces, Solid-State Electron. 15 (5) (1972) 559–571.

[17] E. Borchi, M. Bruzzi, S. Pirollo, S. Sciortino, Temperature and frequency dependence of the capacitance of heavily irradiated silicon diodes, Solid-State Electron. 42 (11) (1998) 2093–2096.

[18] K.H. Zainninger, A.G. Holmes-Siedle, A survey of radiation effect in metal–insulator–semiconductor devices, RCA Rev. (1967) 208–239.

[19] P.S. Winokur, J.M. McGarrity, H.E. Boesch, Dependence of interface-state buildup on hole generation and transport in irradiated MOS capacitors, IEEE Trans. Nucl. Sci. NS-23 (1976) 1580–1585.

[20] G.W. Hughes, Interface-state effects in irradiated MOS structures, J. Appl. Phys. 48 (12) (1977) 5357–5359.

[21] M.R. Chin, T.P. Ma, Gate-width dependence of radiation-induced interface traps in metal/SiO_2/Si devices, Appl. Phys. Lett. 42 (10) (1983) 883–885.

[22] K. Naruke, M. Yoshida, K. Maeguchi, H. Tango, Radiation-induced interface states of poly-Si gate MOS capacitors using low temperature gate oxidation, IEEE Trans. Nucl. Sci. NS-30 (6) (1983) 4054–4058.

[23] P.S. Winokur, J.R. Schwank, P.J. McWhorter, P.V. Dressendorfer, D.C. Turpin, Correlating the radiation response of MOS capacitors and transistors, IEEE Trans. Nucl. Sci. NS-31 (6) (1984) 1453–1460.

[24] E.F. da Silva Jr., Y. Nishioka, T.P. Ma, Radiation response of MOS capacitors containing fluorinated oxides, IEEE Trans. Nucl. Sci. NS-34 (6) (1987) 1190–1195.

[25] J.R. Schwank, P.S. Winokur, et al., Radiation-induced interface-state generation in MOS devices, IEEE Trans. Nucl. Sci. NS-33 (6) (1986) 1178–1184.

[26] T.P. Ma, Interface trap transformation in radiation or hot-electron damaged MOS structures, Semicond. Sci. Technol. 4 (1989) 1061–1079.

[27] A. Candelori, A. Paccagnella, M. Cammarata, G. Ghidini, M. Ceschia, Electron irradiation effect on thin MOS capacitors, J. Non-Cryst. Solids 245 (1999) 238–244.

[28] R.K. Chauhan, P. Chakrabarti, Effect of ionizing radiation on MOS capacitors, Microelectron. J. 33 (2002) 197–203.

[29] M. Walters, A. Reisman, The distribution of radiation-induced charged defects and neutral electron traps in SiO_2, and the threshold voltage shift dependence on oxide thickness, J. Appl. Phys. 67 (1990) 2992–3002.

[30] C. Fanggao, G.A. Saunders, E.F. Lambson, R.N. Hampton, G. Carini, G.D. Marco, M. Lanza, Temperature and frequency dependencies of the complex dielectric constant of poly(ethylene oxide) under hydrostatic pressure, J. Poly. Sci. 34 (1996) 425–433.

[31] E.H. Nicollian, J.R. Brews, MOS (Metal/Oxide/Semiconductor) Physics and Technology, Wiley, New York, 1982.

[32] R. Castagne, A. Vapaille, Description of the SiO_2–Si interface properties by means of very low frequency MOS capacitance measurements, Surf. Sci. 28 (1) (1971) 157–193.

[33] C.T. Sah, Origin of interface states and oxide charges generated by ionizing radiation, IEEE Trans. Nucl. Sci. 23 (1976) 1563–1568.

[34] S. Kar, S. Varma, Determination of silicon–silicon dioxide interface state properties from admittance measurements under illumination, J. Appl. Phys. 58 (11) (1985) 4256–4266.

[35] A. Tataroğlu, Ş. Altındal, S. Karadeniz, N. Tuğluoğlu, Au/SnO_2/*n*-Si (MOS) structures response to radiation and frequency, Microelectron. J. 34 (2003) 1043–1049.

[36] A.A. Sattar, S.A. Rahman, Dielectric properties of rare earth substituted Cu–Zn ferrites, Phys. Status Solidi A 200 (2003) 415–422.

[37] K.S. Moon, H.D. Choi, A.K. Lee, K.Y. Cho, H.G. Yoon, K.S. Suh, Dielectric properties of epoxy-dielectrics-carbon black composite for phantom materials at radio frequencies, J. Appl. Poly. Sci. 77 (2000) 1294–1302.

[38] Z. Jiwei, Y. Xi, W. Mingzhong, Z. Liangying, Preparation and microwave characterization of $PbTiO_3$ ceramic and powder, J. Phys. D: Appl. Phys. 34 (2001) 1413–1416.